Calculation of the Effective Ionization Rate in Air by Considering Electron Detachment From Negative Ions

Journal Article

Author(s):
Chachereau, Alise ; Pancheshnyi, Sergey

Calculation of the effective ionization rate in air taking into account electron detachment from negative ions

Alise Chachereau and Sergey Pancheshnyi

ABB Corporate Research, Segelhofstrasse 1K

5405 Baden-Dättwil, Switzerland

Abstract—The effective Townsend ionization coefficient in dry air at different pressures and temperatures is calculated taking into account ionization by direct electron impact, attachment of electrons to molecular oxygen, simplified negative ion kinetics and detachment of electrons from negative ions in collisions with heavy neutrals. Effect of electron detachment from negative ions created by primary and secondary electron avalanches propagating in a uniform electric field in air at different pressures and temperatures, and its contribution into the effective ionization rate are analyzed.

Index Terms—Air, electron swarm parameters, effective ionization rate, electron detachment, ion kinetics.

I. Introduction

ELECTRON swarm parameters include the transport properties of electrons (mobility and diffusion coefficients) and the rates of kinetic processes (typically, ionization and attachment). In thermal plasmas, near-Maxwellian distribution of electrons allows using relatively simple approaches for calculation of swarm parameters (often, only transport coefficients). In non-thermal plasmas, electron energy distribution can be strongly non-Maxwellian that often has significant impact on electron swarm parameters. Higher values of electric field lead usually to more pronounced discrepancy between the two cases.

Experimentally measured electron swarm parameters are typically only available for simple cases (room temperature, low pressures, simple mixtures — see, for example, one of the most complete survey of electron swarm data by Dutton [1]) and theoretical extension of these data to more complex cases often remains the only feasible approach. Among different possible techniques, solving the Boltzmann equation for the electron energy distribution with the so-called "two-term approximation" remains the most developed and the most used nowadays.

To explain the use of the effective ionization coefficient, the simplest example is that of an electron avalanche. When a uniform electric field is applied to a gas containing some free electrons, these are accelerated and gain kinetic energy. If the field is high enough, the electrons gain sufficient energy between collisions to cause ionization on impact with neutral

S. Pancheshnyi is the contact author, e-mail: sergey.pancheshnyi@ch.abb.com.

A. Chachereau is now at the High Voltage Laboratory of ETH Zurich (e-mail: alisec@ethz.ch).

molecules. In this case, the number of electrons grows exponentially with the distance. This is called a Townsend electron avalanche (Figure 1, top row). The collisions between particles can result in other elementary processes than ionization, for instance, an electron can attach to a neutral particle and create a negative ion. Here is the list of key elementary processes which typically occur in a discharge:

- **Elastic collision** of an electron with heavy species. As a result, the electron transfers a part of its kinetic energy to the other colliding partner. This loss of kinetic energy equals to $2m/M$ where m is the mass of the electron and M that of the species. Since the mass ratio is at most 10^{-4}, the loss of energy is small. The main result of elastic collisions is the Maxwellisation of the electron distribution.
- **Ionization:** If the electron has sufficient energy when it collides with a neutral particle, it can create a positive ion and an additional free electron. It is possible to define a coefficient of ionization α corresponding to the mean number of ionization processes over the distance covered in the direction of the electric field. α is called the first Townsend, or ionization, coefficient.
- **Excitation:** During collision, an electron can also transfer some energy to the particle by exciting it to a higher level of energy in a collision. There are many types of excitation, for instance rotational, vibrational and electronic excitation. Molecular dissociation can also be considered as an excitation process.
- **Attachment:** Electrons can also attach to a neutral particle to create negative ions. This process reduces the number of free electrons in the gas. Similar to ionization, a coefficient characterizing the rate of attachment η is often used.
- **Detachment:** Upon collision of the negative ions with other particles, the captured electrons can be freed again (collisional detachment). Detachment from unstable negative ions can also occur spontaneously (autodetachment).

Since ionization and detachment increase the number of electrons while attachment decreases it, the effective coefficient accounting for the growth of the number of electrons N_e with distance x is the balance between these different processes. It is common to assume that the growth of the number of electrons is still exponential, and to introduce the
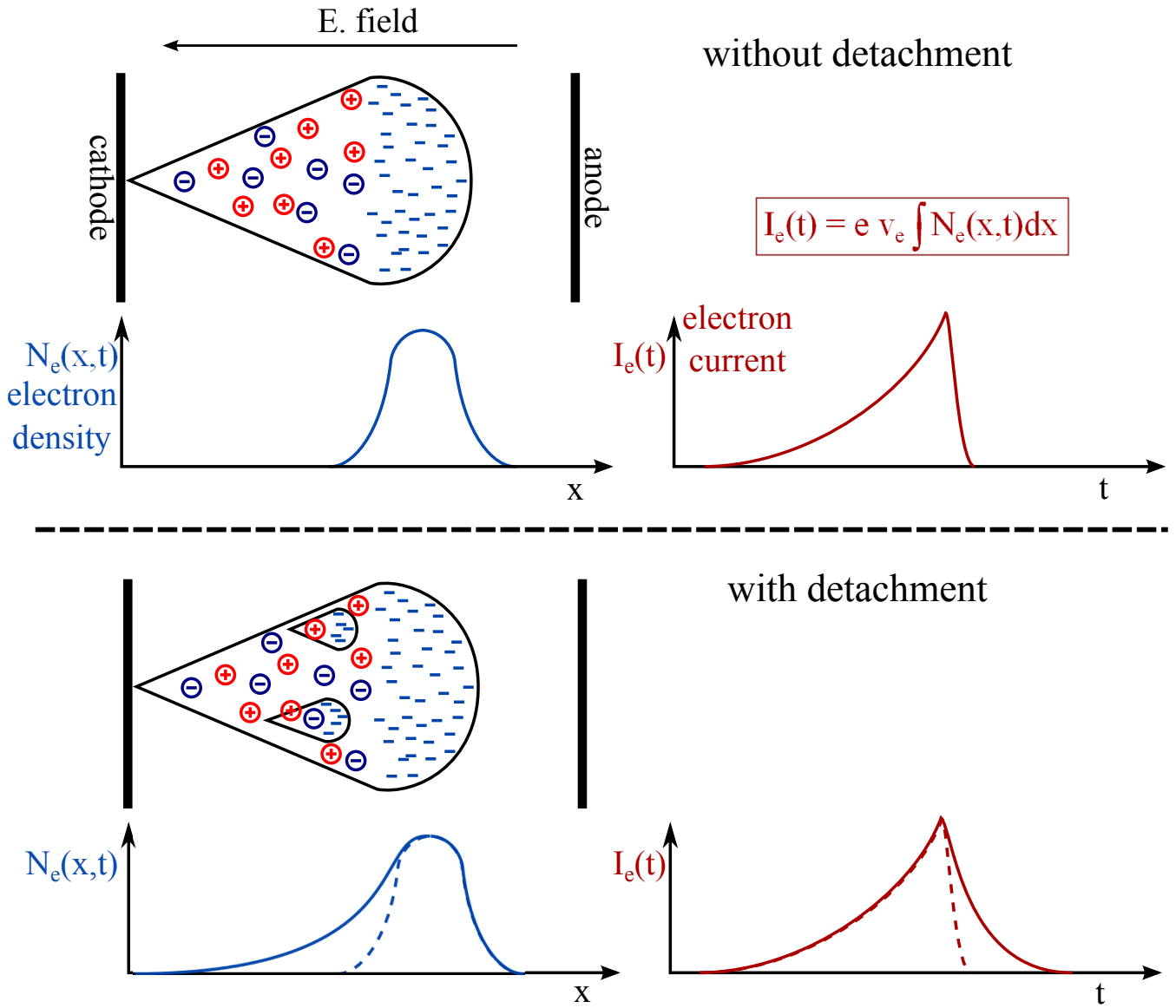
Fig. 1. Schematic diagram of an electron avalanche development in non-detaching (top) and detaching (bottom) gases. Corresponding electron density and induced electric current are shown.

effective coefficient of ionization α_{eff}:

$$\frac{dN_e}{dx} = \alpha_{eff} N_e, \qquad (1)$$
$$N_e(x) = N_0 \exp(\alpha_{eff} x), \qquad (2)$$

where the effective coefficient α_{eff} is the result of all relevant processes.

In electropositive gases like argon and nitrogen, there is no attachment and, therefore, the growth of the number of electrons is only due to collisional ionization, i.e. $\alpha_{eff} = \alpha$. In electronegative gases, such as air, attachment and detachment from negative ions can additionally occur. Publications (see, for example, [2]) often take into account only collisional ionization α and attachment of electrons to heavy neutrals η in the following way

$$\alpha_{eff} = \alpha - \eta. \qquad (3)$$

However, electron detachment from negative ions can also have impact on the ionization rate. For instance, it is known that detachment in air can be important at temperatures above 2'000 K due to the presence of atomic oxygen in the gas [3], [4]. On the other hand, it was shown in [5] that another mechanism of detachment from negative ions and eventual negative ion conversion has also significant impact, especially at elevated electric fields. Detached electrons generate delayed secondary avalanches following the path of the first avalanche (Figure 1, bottom row) and can contribute significantly to the total amount of charge transferred as it has been experimentally shown in [6]. Although these detachment mechanisms are fairly well known, they are rarely taken into account for determination of electron swarm parameters. One of the method used, for example, in [3] describes approximately the
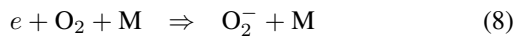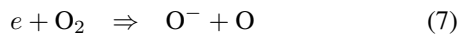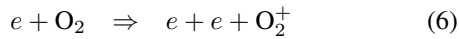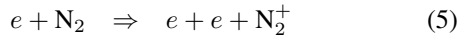
rate of multiplication of electrons as

$$\alpha_{eff} = \alpha - \frac{\eta}{1 + \nu_{det}/\nu_{att}}, \qquad (4)$$

where ν_{att} and ν_{det} are the attachment and the detachment frequencies, respectively. While this formula gives the correct values in both limiting cases ($\nu_{att} \gg \nu_{det}$ and $\nu_{att} \ll \nu_{det}$), its generalization to intermediate situations remains unclear. The aim of this work is to evaluate the influence of detachment, to give simple directives for determining in which cases it should be taken into account, and to develop a model to calculate the effective ionization coefficient in dry air (simplified as a mixture of 80% nitrogen and 20% oxygen) in a wide pressure and temperature range. It gives a model to calculate the effective ionization coefficient, taking into account these two detachment mechanisms, and separate models for evaluating their respective contribution. The same approach can be applied for other gases as well, knowing detailed kinetics of negative ions.

II. KINETICS OF CHARGED SPECIES

A. Basic model with ionization and attachment only

The main processes of ionization and attachment in cold air are

$$
\begin{align}
e + N_2 &\Rightarrow e + e + N_2^+ \qquad &(5) \\
e + O_2 &\Rightarrow e + e + O_2^+ \qquad &(6) \\
e + O_2 &\Rightarrow O^- + O \qquad &(7) \\
e + O_2 + M &\Rightarrow O_2^- + M \qquad &(8)
\end{align}
$$

where M is any heavy species (N_2 and O_2, essentially). Similarly, collisions of electrons with other species (N and O atoms, NO molecules, etc.) leading to ionization and attachment have to be included at high temperatures. Ionization increases the number of electrons while attachment decreases it. As a result, the number densities of electrons N_e, negative ions N_n and positive ions N_p obey the following system of balance equations

$$
\begin{align}
\frac{dN_e}{dx} &= \alpha N_e - \eta N_e \qquad &(9) \\
\frac{dN_n}{dx} &= \eta N_e \qquad &(10) \\
\frac{dN_p}{dx} &= \alpha N_e \qquad &(11)
\end{align}
$$

where α is the ionization coefficient and η is the attachment coefficient. These equations are not coupled, so the solution for the number density of electrons can be expressed in exponential form (2) with the effective ionization coefficient (3).

In the present work, an approach is developed for calculating electron swarm parameters using the solver BOLSIG+, coupled with the package Cantera for calculating the gas composition at chemical equilibrium. An interface written in Python language is used for the coupling of the two solvers. The gas composition at given pressure and temperature is determined with Cantera and sent to BOLSIG+, which returns the electron swarm parameters α, η, v_e, etc. in required text

and graphical formats (see Figure 2). Since the detachment processes will be considered in following sections separately from ionization and attachment, the influence of detachment on the electron energy distribution is considered, although it might change the final result. Meanwhile, significant uncertainty in kinetic processes and corresponding reaction rates can have a more important impact on the overall accuracy of the model.

B. Calculation of swarm parameters using Boltzmann solver

There are a few solvers of Boltzmann equation available commercially or distributed as freeware. BOLSIG+ software [7], being a significantly improved successor of BOLSIG package [8], was developed to obtain the electron transport coefficients and collision rate coefficients from scattering cross section data for electrons in weakly ionized gases in uniform electric fields, conditions which typically appear in the bulk of collisional low-temperature plasmas. Nowadays, the solver is available as a standalone Windows application [9], as online solver at LXCAT project [10] and pre-compiled library in ZDPLASKIN package [11] (used in this work).

Electron collisions with chemical species involved in the processes are characterized by scattering cross sections, which correspond to the probability to collide with these particles. The effective cross section of a species can only be experimentally determined or calculated from first principals for simple atoms (see [12]–[14] and references therein for details).

The LXCAT project [10], [15] offers probably the most comprehensive collection of complete sets of cross sections for electron scattering with neutral atoms and molecules from ground state to some hundreds of eV and higher. Complete sets of cross sections, consisting of elastic momentum transfer and total cross sections for the processes of ionization, attachment and excitation, are needed as input to a Boltzmann equation solver to determine the electron or ion energy distribution function. The data used in this work was retrieved from Phelps [16] and SIGLO [17] databases.

Figure 3 shows the results obtained for the reduced ionization coefficient α/N and the effective reduced ionization coefficient $(\alpha - \eta)/N$ as functions of reduced electric field E/N at 300 K. The cut-off in the curve $(\alpha - \eta)/N$ corresponds to the critical field (approximately 120 Td in this case). Note, the reduced electric field E/N, i.e. the electric field E over the gas density N, is mostly used in this work. The corresponding unit is Td (1 Td = 10^{-17} V cm^2) as commonly used in plasma community.

The electron distribution is obtained by BOLSIG+ from the balance between electric acceleration and momentum loss and energy loss in collisions with neutral gas particles approximating the angular dependence of the distribution by the classical two-term expansion. Using these assumptions, the Boltzmann equation simplifies into a convection-diffusion continuity equation with a non-local source term in energy space [7].

At a sufficiently high reduced electric field, a fraction of electrons pass to a mode of continuous acceleration (so-called "runaway electrons"), so that the two term approximation is not
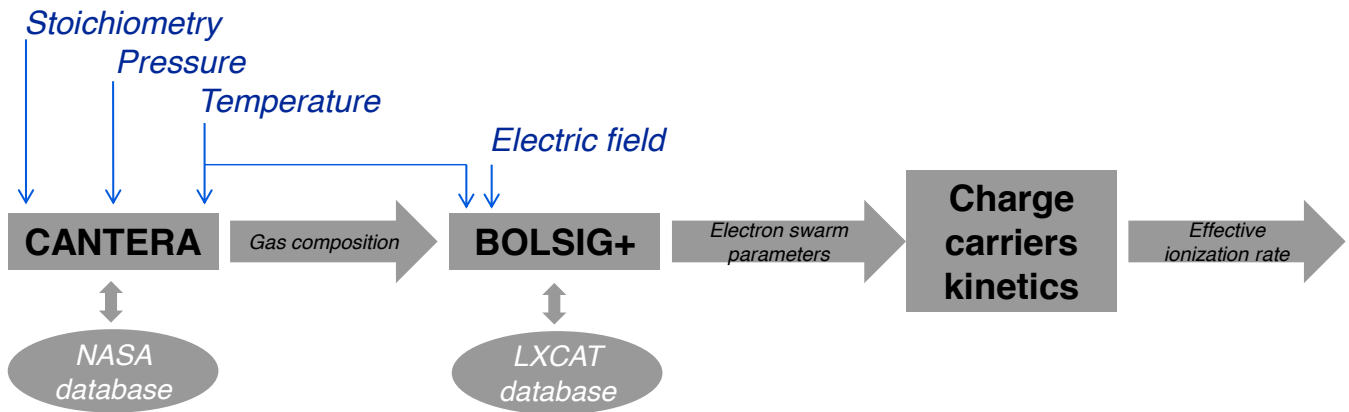
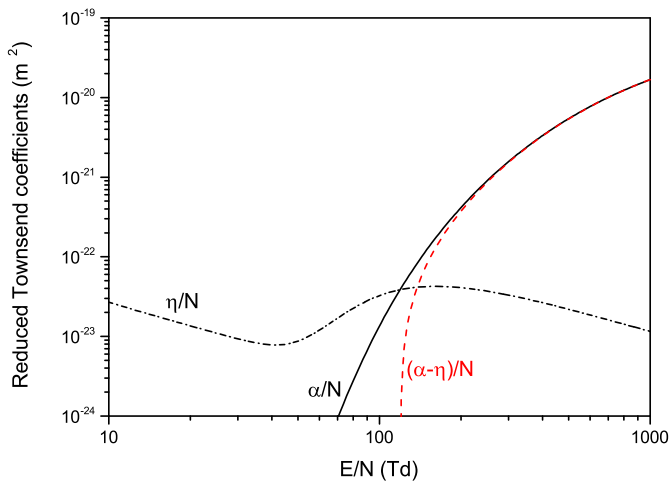Fig. 2. Flowchart of the calculations.

Fig. 3. Gas-density reduced ionization rate α/N, attachment rate η/N and their difference $(\alpha - \eta)/N$ as functions of the reduced electric field E/N in air at 1 bar and 300 K.
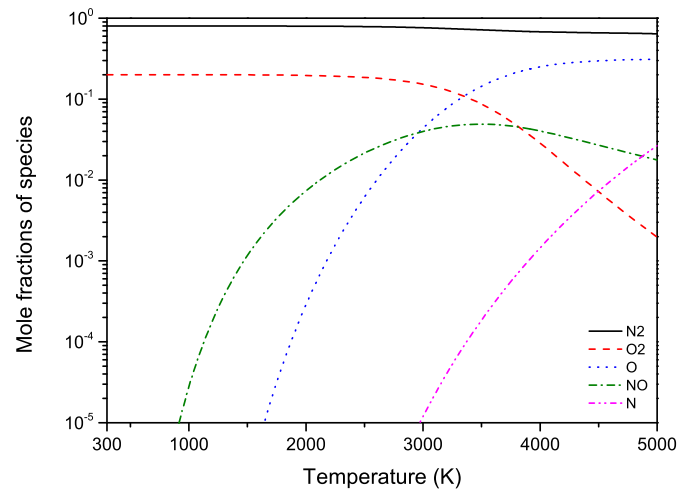

Fig. 4. Equilibrium composition of dry air at atmospheric pressure as a function of gas temperature.

valid. For nitrogen, the critical field where electron runaway is possible was estimated to be about 2'000 Td [18]. At lower reduced fields, typically below 1'000 Td, calculations of swarm parameters in molecular gases yield generally good agreement with measurements [19], [20].

C. Influence of gas temperature and pressure

At low temperatures, air is mainly constituted of N_2 and O_2. However, at higher temperatures, dissociation of these species leads to remarkable concentrations of other species (O, N, NO, etc). The composition of gas can be calculated using a thermodynamic approach in the LTE case. It consists in minimizing the Gibbs function for the mixtures of all stable species containing N and O atoms under given pressure and temperature. This calculations are done here using Cantera package, an open-source, object-oriented software package developed by a team from California Institute of Technology which performs chemical and thermodynamic equilibrium and kinetics calculations [21].

Thermodynamic data are necessary for performing equilibrium chemistry calculations. These data typically provide the thermodynamic properties (enthalpy, entropy and specific heat) of a species as a function of temperature. Cantera includes the NASA thermodynamic database (`nasa.cti` file) which is used in this work. The thermodynamic properties for most species in the database are only suitable for gas temperatures up to 6'000 K.

As an example, Figure 4 shows the mole fractions of the main species in air for temperatures between 300 K and 5'000 K at atmospheric pressure.

The change in gas composition affects the swarm parameters, because the cross sections of the new species are different. For example, Figure 5 shows the effective ionization coefficient $(\alpha - \eta)/N$ for various temperatures in 300–4'000 K range. As it follows from the Figure, the critical field monotonously decreases when the temperature increases.

D. Collisional detachment on O atoms

At elevated temperatures the presence of atomic oxygen in the gas leads to strong detachment from oxygen negative ions
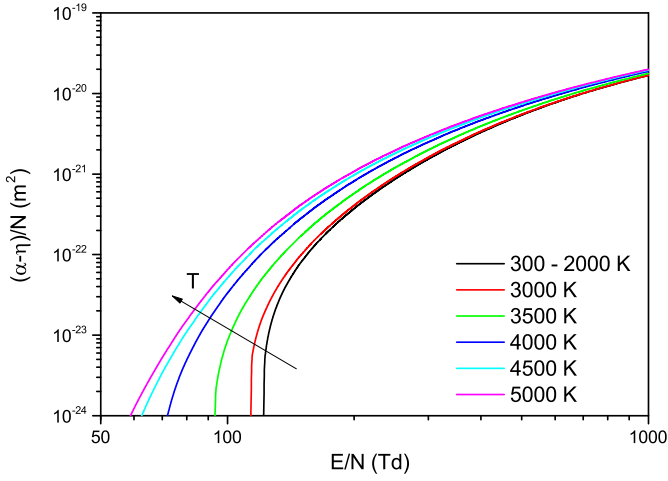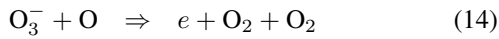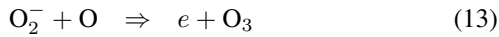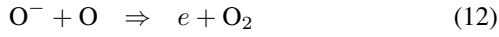
Fig. 5. $(\alpha - \eta)/N$ as a function of reduced electric field E/N for different temperatures in air at 1 bar.

[3], [4]. The main processes are the following

$$O^- + O \quad \Rightarrow \quad e + O_2 \qquad (12)$$

$$O_2^- + O \quad \Rightarrow \quad e + O_3 \qquad (13)$$

$$O_3^- + O \quad \Rightarrow \quad e + O_2 + O_2 \qquad (14)$$

Similarly to the ionization and attachment coefficients, a detachment coefficient δ can be introduced. The set of equations determining the number densities of electrons N_e, negative ions N_n and positive ions N_p then becomes

$$\frac{dN_e}{dx} = \alpha N_e - \eta N_e + \delta N_n \qquad (15)$$

$$\frac{dN_n}{dx} = \eta N_e - \delta N_n \qquad (16)$$

$$\frac{dN_p}{dx} = \alpha N_e \qquad (17)$$

These equations are coupled, but assuming the solution to be exponential as in (1), it is possible to get an analytical expression for the effective ionization coefficient corresponding to this detachment mechanism

$$\alpha_{eff}^2 + \alpha_{eff}(\eta - \alpha + \delta) - \delta\eta + \delta(\eta - \alpha) = 0. \qquad (18)$$

The analytical solution for α_{eff} is the positive root of this second-order polynomial equation (see also [5])

$$\alpha_{eff} = \frac{1}{2}\left(\alpha - \eta - \delta + \sqrt{(\eta - \alpha - \delta)^2 + 4\delta\eta}\right). \qquad (19)$$

We limit here the range of considered values $\alpha_{eff} \geq 0$. Indeed, negative values correspond to the cases of quick quenching of avalanches and has very limited interest for this work. Note that detachment can only compensate partially attachment, it can not produce more electrons than there are negative ions. Therefore the upper limit for the effective ionization coefficient is the ionization coefficient α/N, and the lower limit is $(\alpha - \eta)/N$. The constant rates of reactions (12) – (14) and the mobility of the negative ions are given in Tables I and II, respectively. Since the ratio of constant rate to mobility is very

TABLE I
CONSTANT RATES FOR COLLISIONAL DETACHMENT ON O ATOMS IN CM^{3}S^{-1}, RETRIEVED FROM [4].

k_{12}	1.4×10^{-10}
k_{13}	1.5×10^{-10}
k_{14}	3×10^{-10}

TABLE II
ION REDUCED MOBILITY AT $E/N = 100$ TD IN M^{-1}V^{-1}S^{-1}, RETRIEVED FROM [22] (SEE ALSO [5]).

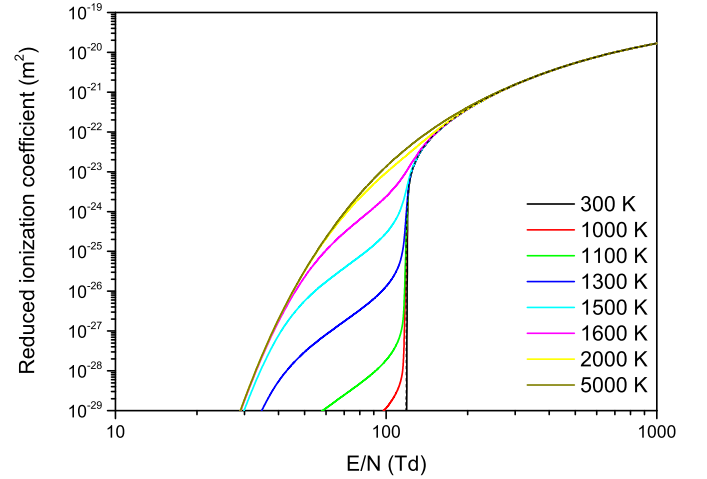|	
$\mu_{O^-}N$	1.2×10^{22}
$\mu_{O_2^-}N$	7.1×10^{21}
$\mu_{O_3^-}N$	7.6×10^{21}

Fig. 6. α_{eff}/N as a function of the reduced electric field for different temperatures in air at 1 bar. Ionization, attachment and detachment on O atoms is included, equation (19).

close for the three ions, the averaged detachment coefficient δ is taken here as

$$\delta = \frac{k_{13}}{v_{O_2^-}}[O], \qquad (20)$$

where $v_{O_2^-} = \mu_{O_2^-}E$ is the drift velocity of O_2^- ions in electric field and $[O]$ is the density of O atoms.

Figure 6 shows the curves of the effective ionization coefficient reduced through gas density α_{eff}/N taking into account collisional detachment on atomic oxygen, as a function of the reduced electric field and at different temperatures. This result shows that detachment has significant impact on the effective ionization coefficient. It can be seen that for temperatures above 2'000 K, the detachment compensates almost completely attachment losses and the effective ionization coefficient essentially equals to the ionization coefficient. At low temperatures however, this detachment mechanism is insignificant because there is little amount of atomic oxygen in the gas.

E. Collisional detachment on N$_2$ and O$_2$ molecules

Collisions of O^- and O_2^- ions with heavy species can also cause important detachment from negative ions in $N_2 - O_2$

mixtures, as described in [5]. The main processes are

$$O^- + N_2 \;\Rightarrow\; e + N_2O \tag{21}$$

$$O_2^- + M \;\Rightarrow\; e + O_2 + M \tag{22}$$
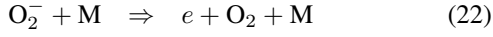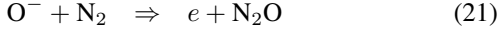
where O^- and O_2^- negative ions are primarily created in processes (7) and (8). Fast negative ion conversion, however, can lead to substantial generation of O_3^- ions as well. It is mainly produced in the following reaction

$$O^- + O_2 + M \;\Rightarrow\; O_3^- + M. \tag{23}$$
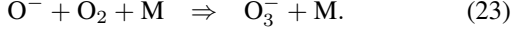
In this detachment mechanism, O_3^- ions hardly contribute to detachment as they did in the previously discussed mechanism. Therefore in this case two types of negative ions are introduced as suggested in [6]. The ions that contribute to detachment (here O^- and O_2^-) are called unstable negative ions (un), and the ions that do not contribute to detachment (O_3^-) are called stable negative ions (sn).

By introducing a detachment coefficient δ and a coefficient of conversion into stable negative ions ω, it is possible to rewrite the set of equations for the number densities of the different charged species (electrons N_e, unstable negative ions N_{un}, stable negative ions N_{sn}) and positive ions N_p as

$$\frac{dN_e}{dx} = \alpha N_e - \eta N_e + \delta N_{un} \tag{24}$$

$$\frac{dN_{un}}{dx} = \eta N_e - \delta N_{un} - \omega N_{un} \tag{25}$$

$$\frac{dN_{sn}}{dx} = \omega N_{un} \tag{26}$$

$$\frac{dN_p}{dx} = \alpha N_e \tag{27}$$

and proceeding similarly as in the previous section, it is again possible to get the analytical solution for α_{eff} as the positive root of a second order polynomial equation (see also [5])

$$\alpha_{eff} = \frac{1}{2}\left(\alpha - \eta - \delta - \omega + \sqrt{(\eta - \alpha - \delta - \omega)^2 + 4\delta\eta}\right). \tag{28}$$

The total detachment coefficient δ corresponding to reactions (21) – (22) is

$$\delta = \frac{k_{21}}{v_{O^-}}[N_2] + \frac{k_{22}}{v_{O_2^-}}N, \tag{29}$$

where k_{21} and k_{22} are the constant rates of reactions (21) and (22).

In addition to introducing a detachment coefficient, this mechanism requires to introduce the coefficient of conversion into stable negative ions ω according to process (23):

$$\omega = \frac{k_{23}}{v_{O^-}}[O_2]N, \tag{30}$$

where k_{23} is the constant rate of reaction (23). As shown in [5], the reaction rates k_{21} and k_{22} can be approximated with an Arrhenius function

$$k_i = k_i^0 \exp\left(-\frac{\Delta\epsilon_i}{\theta_{ion}}\right), \tag{31}$$

where k_i^0 is the pre-exponential factor for reaction i, $\Delta\epsilon_i$ is the activation energy of the reaction and θ_{ion} is the characteristic temperature of the ions

$$\theta_{ion} = \frac{\pi}{2}m_{ion}v_{ion}^2 + T_{gas}, \tag{32}$$

TABLE III
CONSTANT RATES AND ACTIVATION ENERGIES, RETRIEVED FROM [5].

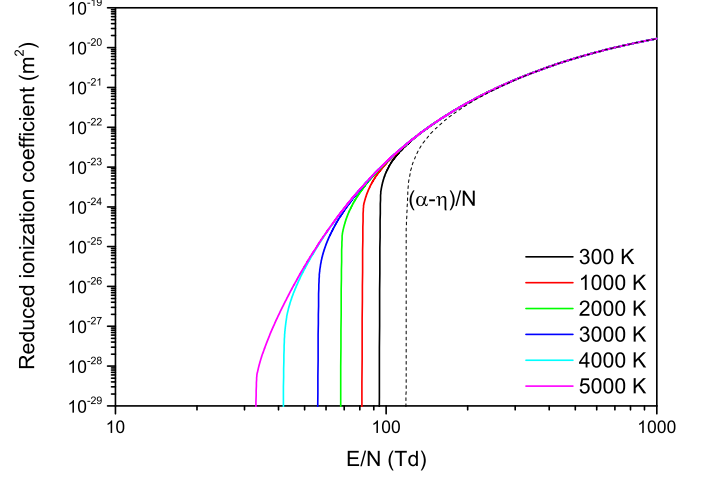| k_i^0		$\Delta\epsilon_i$		
1.16×10^{-12}	cm^{3}s^{-1}	0.076	eV	(21)
1.22×10^{-11}	cm^{3}s^{-1}	0.78	eV	(22)
1.3×10^{-30}	cm^{6}s^{-1}	0.16	eV	(23)

Fig. 7. α_{eff}/N as a function of the reduced electric field for different temperatures in air at 1 bar. Ionization, attachment and detachment on N_2 and O_2 molecules is included, equation (28).

with T_{gas} expressed in eV. The reaction rate k_{23} has different dependency according to [5]

$$k_i = k_i^0 \exp\left(-\frac{\theta_{ion}}{\Delta\epsilon_i}\right). \tag{33}$$

Corresponding values of k_i^0 and $\Delta\epsilon_i$ proposed in [5] are summarized in Table III.

Figure 7 shows the effective ionization coefficient at different temperatures taking into account the collisional detachment on N_2 and O_2 molecules as a function of reduced electric field. In the Figures, the dashed curve is the $(\alpha - \eta)/N$ difference at 300 K representing the commonly used value for effective ionization rate. As it follows from the Figure, this detachment mechanism has strong influence on the effective ionization coefficient at all temperatures.

Note that grouping O^- and O_2^- ions into one unstable ion is valid because of the fast ion conversion

$$O^- + O_2 \Rightarrow O_2^- + O \tag{34}$$
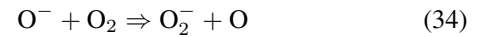
and the decreasing rate of O_3^- ion formation (23) with increasing reduced electric field (33). For low fields, $E/N \lesssim 50$ Td at normal conditions according to Figure 3, this assumption can overestimate the rate of O_3^- production, and thus underestimate collisional detachment, because the conversion takes place only for O^- ions in process (23) while O_2^- is the dominant negative ion created in process (8). However, this range of reduced fields remains below the critical field for this detachment mechanism at low temperatures (see Figure 7) while detachment on O atoms (12-14) dominates at higher gas temperatures. Thus, the grouping of O^- and O_2^- into one
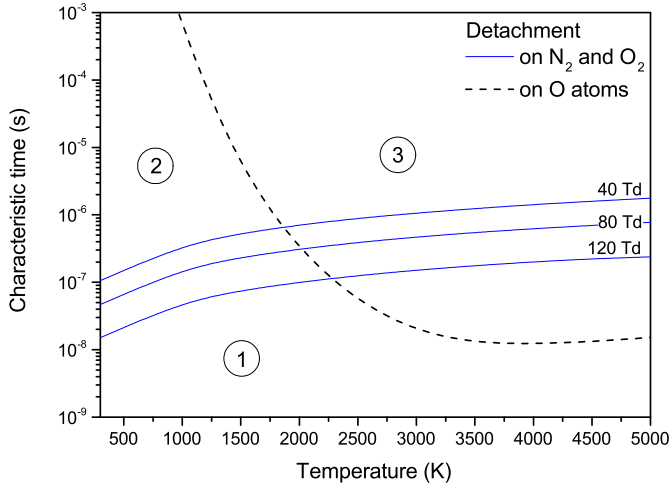
Fig. 8. Characteristic time of detachment processes in air at 1 bar.

Fig. 9. Schematic of the production of the different charged species, taking into account ionization (α), attachment (η), ion conversion (ω), detachment from unstable (δ_{un}) and from stable negative ions (δ_{sn}).

unstable ion has a little overall impact on the accuracy of the model.

F. Dominant detachment mechanism

The mechanisms of detachment on atomic oxygen and with N_2 and O_2 molecules have certain characteristic times respectively given by

$$\tau_O = \frac{1}{k_{13}[O]} \tag{35}$$

$$\tau_{N_2/O_2} = \frac{1}{k_{21}[N_2] + k_{22}N} \tag{36}$$

where τ_O is a function of the gas temperature only while τ_{N_2/O_2} is a function of the temperature and the electric field. Figure 8 shows τ_O and τ_{N_2/O_2} as functions of the temperature. At low temperatures, collisional detachment on N_2 and O_2 molecules is much faster than with atomic oxygen, so the detachment from collisions with N_2 and O_2 is dominant. For higher temperatures both mechanisms should be considered.

The interpretation of these curves allows to judge whether or not detachment should be taken into account in a given application. One needs to know the characteristic time and temperature range of the application, and to place it on the graph.

The curves delimit three regions. If the application is in region (1) the application is so fast that detachment has no time to happen and can be neglected. In that case the effective ionization coefficient is simply that given by (3).

If the application is in region (2) only detachment on N_2 and O_2 molecules should be taken into account. In that case the effective ionization coefficient is given by (28).

If the application is in region (3) both detachment mechanisms have ample time to happen and should be taken into account. In that case the effective ionization coefficient is given by the complete numerical model which will be presented in the next section.
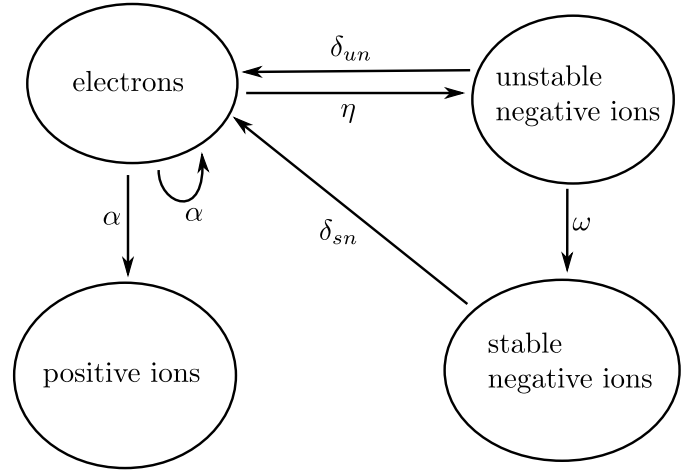
III. NUMERICAL SOLUTION OF THE COMPLETE SYSTEM

Two types of negative ions have been introduced, reflecting the different mechanism of electron detachment from these ions. Reactions (12), (13), (21), (22) participate to detachment from unstable negative ions (δ_{un}) while process (14) corresponds to detachment from stable negative ions (δ_{sn}). Schematic diagram 9 represents the production ways of main charged species. The number densities of the charged species obey the following complete system of balance equations

$$\frac{dN_e}{dx} = \alpha N_e - \eta N_e + \delta_{un}N_{un} + \delta_{sn}N_{sn} \tag{37}$$

$$\frac{dN_{un}}{dx} = \eta N_e - \omega N_{un} - \delta_{un}N_{un} \tag{38}$$

$$\frac{dN_{sn}}{dx} = \omega N_{un} - \delta_{sn}N_{sn} \tag{39}$$

$$\frac{dN_p}{dx} = \alpha N_e \tag{40}$$

where δ_{un} is the coefficient of detachment from unstable negative ions (O^-, O_2^-), consequently it is the sum of the two detachment coefficients introduced previously

$$\delta_{un} = \frac{k_{13}}{v_{O_2^-}}[O] + \frac{k_{21}}{v_{O^-}}[N_2] + \frac{k_{22}}{v_{O_2^-}}N \tag{41}$$

and δ_{sn} is the coefficient of detachment from stable negative ions (O_3^-), consequently it is the coefficients of collisional detachment on atomic oxygen only

$$\delta_{sn} = \frac{k_{13}}{v_{O_2^-}}[O]. \tag{42}$$

A. Effective ionization coefficient

In principle, similar to previous sections, the effective ionization coefficient is the root of a third order polynomial equation

$$\alpha_{eff}^3 + \alpha_{eff}^2(\delta_{un} + \omega + \eta - \alpha)$$
$$+ \alpha_{eff}(\delta_{sn}(\omega + \delta_{un} - \delta_{sn}) + \eta(\delta_{sn} + \omega) - \alpha(\delta_{un} + \omega))$$
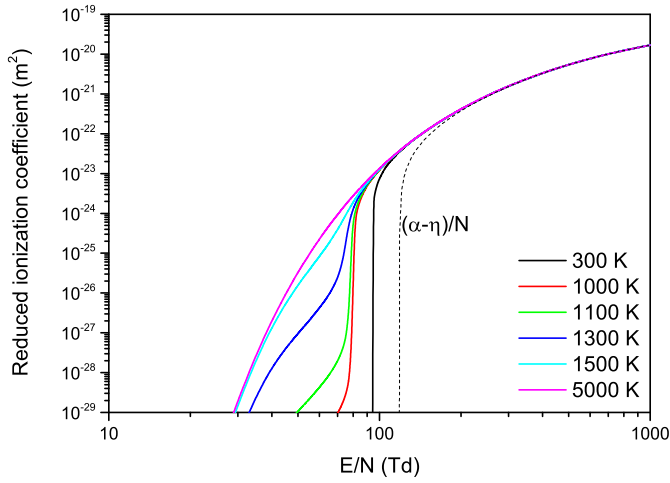$$- \alpha\delta_{sn}(\omega + \delta_{un} - \delta_{sn}) = 0 \tag{43}$$

Fig. 10. α_{eff}/N as a function of the reduced electric field for different temperatures in air at 1 bar. Numerical solution of complete set of processes (37) – (40).
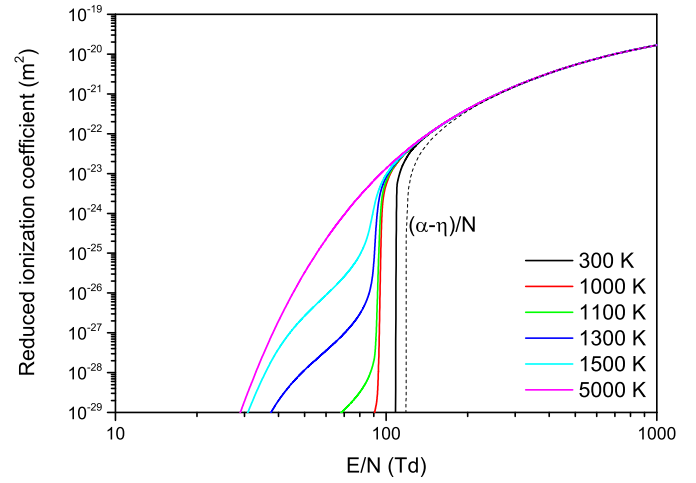

Fig. 12. α_{eff}/N as a function of the reduced electric field for different temperatures in air at 10 bar. Numerical solution of complete set of processes (37) – (40).

Fig. 11. α_{eff}/N as a function of the reduced electric field for different temperatures in air at 0.1 bar. Numerical solution of complete set of processes (37) – (40).
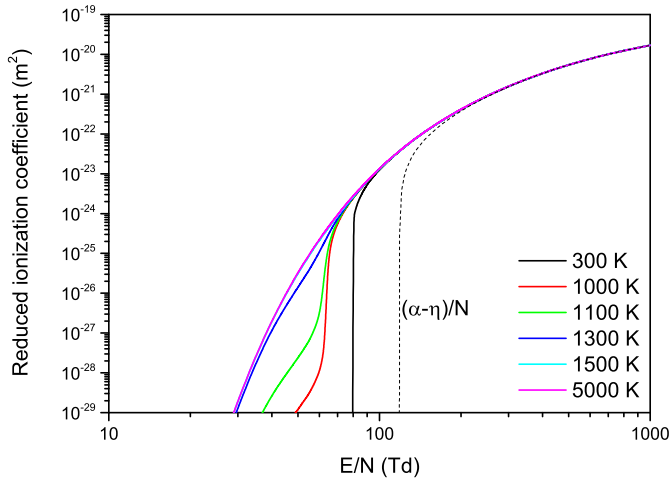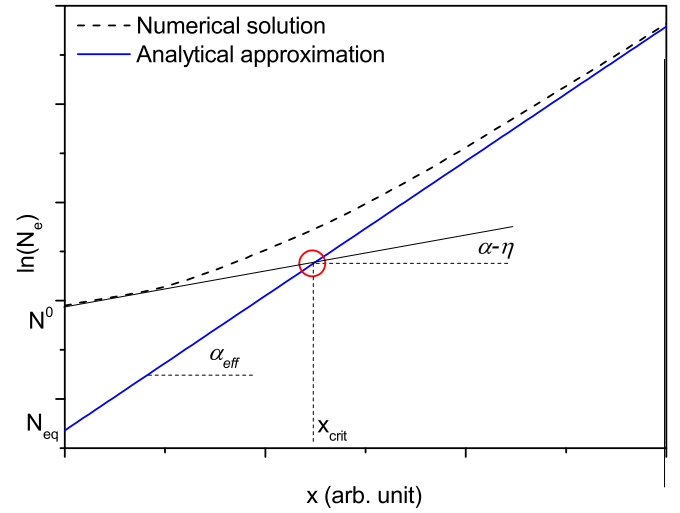

Fig. 13. Growth of the number of electrons: complete numerical solution (37) and analytical approximation (2). x_{crit} is defined as the distance where the analytical and the numerical solutions start to differ by less than 1%.

The solution could be expressed analytically, but it is at least as straightforward to calculate the direct numerical solution of the set of equations (37) – (40).

Figures 10 – 12 show the numerical solution for the effective ionization coefficient (43) taking into account both detachment mechanisms, as a function of the reduced electric field in air at pressures 0.1 – 10 bar at different temperatures.

B. Equivalent initial number of electrons and ions

The results presented in Figures 10 – 12 are obtained assuming that $N_e(x)$ has an exponential form as in formula (2). By numerically solving the system (37) – (40) it can be shown that this assumption is not strictly true. Typical profiles of electron density growth obtained with numerical solution of the complete system and the analytical approximation are plotted in Figure 13. The slope of the numerical solution in the Figure changes from $\alpha - \eta$ at the beginning according to non-detaching case (3) to α_{eff} after a certain distance x_{crit}.

Then, the number density of electrons grows exponentially and the use of effective ionization coefficient (2) is valid. For shorter distances $x < x_{crit}$, such assumption can lead to significant discrepancies (see Figure 13) and direct solution of the complete system (37) – (40) is required.

For longer distances $x > x_{crit}$, the use of analytical form (2) is sufficiently precise. However, the equivalent number of initial electrons N_e^{eqiv} to be used according to

$$N_e(x) = N_e^{eqiv} \exp(\alpha_{eff} x) \qquad (44)$$

can differ from the real number of initial electrons N_e^0, similar to the results presented in Figure 13. Therefore it is important to know the critical distance since it is a limit of the validity domain of this analytical form, and the equivalent number of initial electrons to consider.

Based on direct solution of the set of equations (37) – (40), the critical distance x_{crit} and the equivalent ratio of initial electrons N_e^{eqiv}/N_e^0 to use in the analytical form (44) were
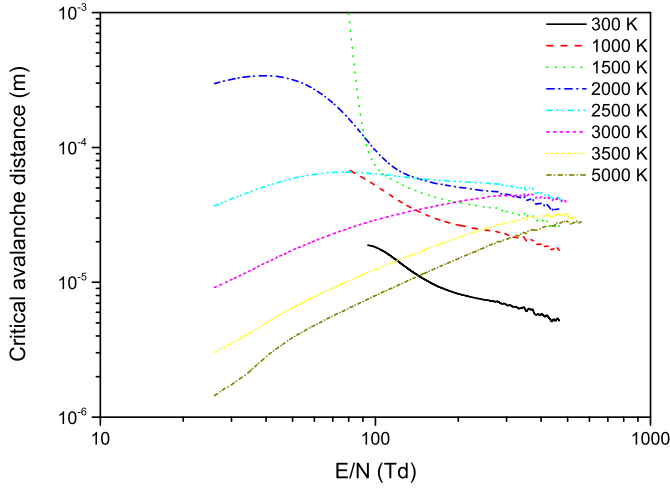
Fig. 14. Critical avalanche distance x_{crit} for different temperatures in air at 1 bar.

Fig. 16. Equivalent ratio of initial electrons to use in the analytical form (44), corresponding to initial unstable negative ion, for different temperatures in air at 1 bar.
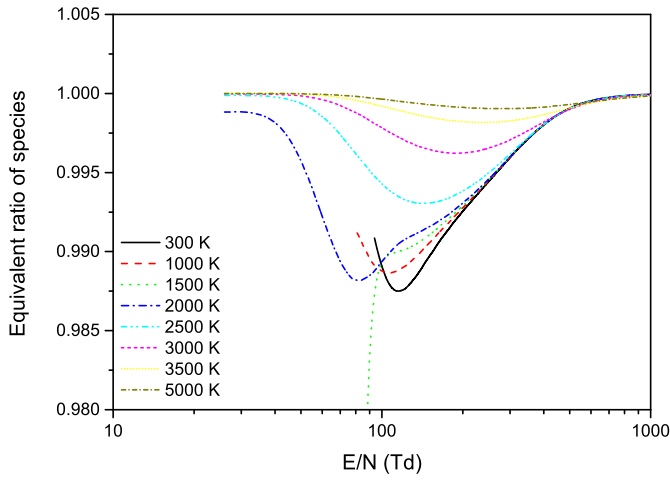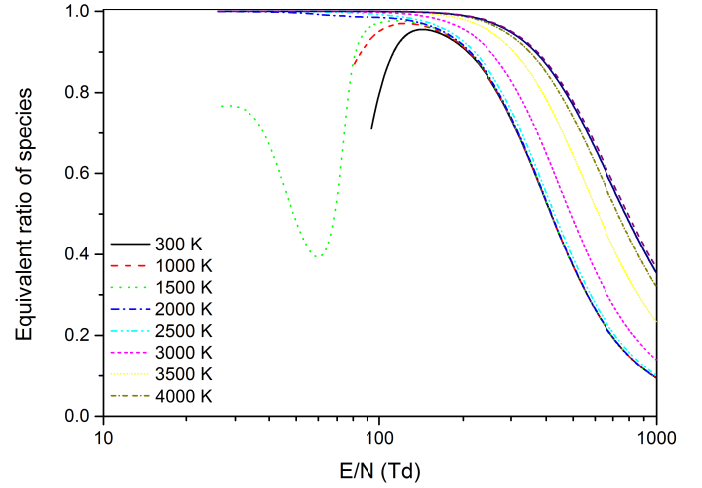

Fig. 15. Equivalent ratio of initial electrons to use in the analytical form (44), corresponding to initial electron, for different temperatures in air at 1 bar.

calculated for the two cases of starting with only electrons (Figures 14 – 15) and starting with only unstable negative ions (Figure 16). As follows from the Figures, the critical distance in both cases remains well below 1 mm. This means the exponential form (44) used in analytical modeling is valid for most typical applications.

According to Figure 15, the equivalent initial number of electrons is close to one. This means the analytical form can be used directly with the initial number of electrons (although it is valid only after the critical distance x_{crit}). In case of initiating avalanche from unstable negative ions (O^-, O_2^-), the equivalent number of initiating electrons variates with temperature and electric field but remains close to one in the most critical field range (100-200 Td) according to Figure 16.

C. Temporal growth of electrons

Kinetic processes can be described by a reaction rate k that is the number of reactions per unit time and per unit volume, but historically Townsend coefficients α, η, δ, etc. — which express the number of reactions per unit length covered by

the electron in the direction of the electric field (considering that the electron moves with the drift velocity v_e) — are used. Therefore the electrons swarm parameters can be expressed either in terms of constant rates which describe the temporal growth of the number of electrons, or in terms of Townsend coefficients describing the spacial growth of the number of electrons.

The same approach as presented previously can be used for describing spacial growth of the number of electrons similar to (2)

$$N_e(t) = N_0 \exp\left(k_{eff} N t\right). \tag{45}$$

The correspondence between the coefficients for spacial growth and temporal growth is following

$$\alpha \;\Rightarrow\; k_{ion} = \alpha v_e / N \tag{46}$$

$$\eta \;\Rightarrow\; k_{att} = \eta v_e / N \tag{47}$$

$$\omega \;\Rightarrow\; k_{conv} = k_{23}[O_2] \tag{48}$$

$$\delta_{un} \;\Rightarrow\; k_{det}^{un} = k_{13}\frac{[O]}{N} + k_{21}\frac{[N_2]}{N} + k_{22} \tag{49}$$

$$\delta_{sn} \;\Rightarrow\; k_{det}^{sn} = k_{13}\frac{[O]}{N} \tag{50}$$

The calculated in this way the effective ionization constant rate k_{eff}, the critical time t_{crit} and the equivalent ratio of initial electrons N_e^{eqiv}/N_e^0 are presented in Figures 17 – 20.

IV. CONCLUSIONS

Effects of electron detachment from negative ions created by primary and secondary electron avalanches propagating in a uniform electric field in air at different pressures and temperatures, and its contribution into the effective ionization rate are studied theoretically in this work.

Kinetics of detachment mechanisms of O^-, O_2^- and, O_3^- ions in collisions with O atoms at elevated gas temperatures and with N_2 and O_2 molecules at all gas temperatures is presented. The values of effective ionization coefficient are obtained and the validity of the method is analyzed. The
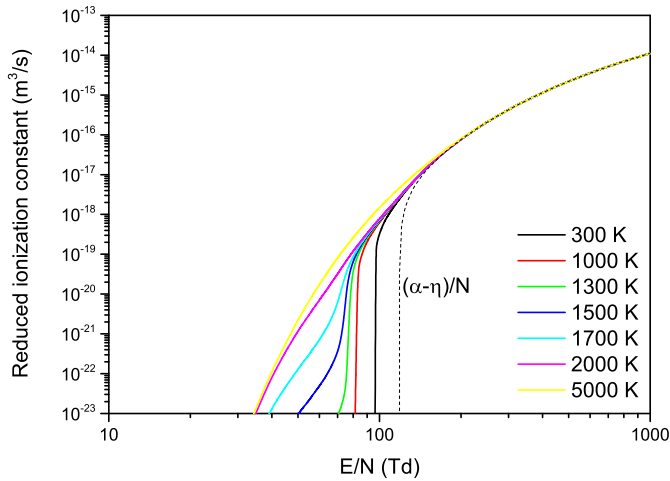
Fig. 17. k_{eff} as a function of the reduced electric field for different temperatures in air at 1 bar. Numerical solution of complete set of processes (37) – (40).

Fig. 18. Critical time as a function of the reduced electric field for different temperatures in air at 1 bar.

Fig. 19. Equivalent ratio of initial electrons to use in the analytical form (45), corresponding to initial electron, for different temperatures in air at 1 bar.
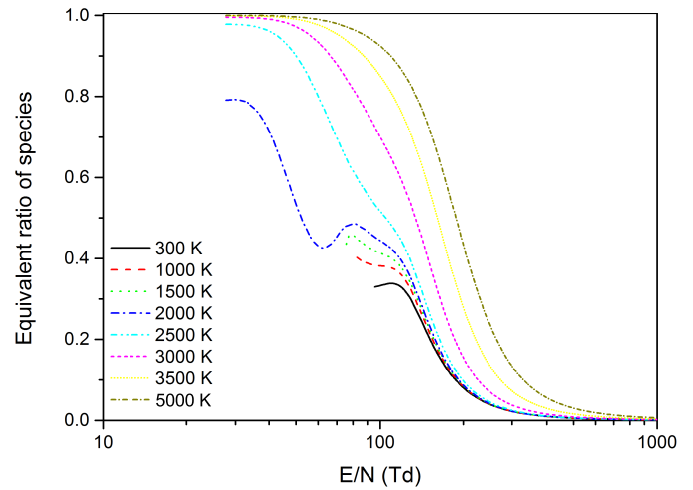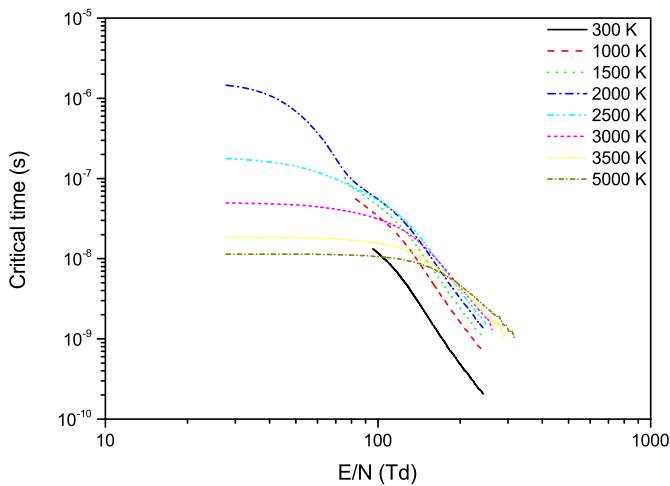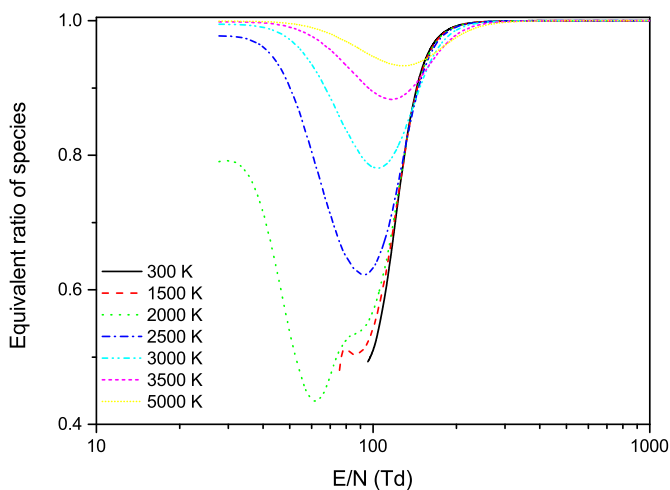

Fig. 20. Equivalent ratio of initial electrons to use in the analytical form (45), corresponding to initial unstable negative ion, for different temperatures in air at 1 bar.

same approach was used to obtain the coefficients describing temporal growth of electrons and the corresponding results are presented for different pressures in the range 0.1-10 bar and 300-5'000 K.

It is shown that electron detachment from negative ions leads to non-zero effective ionization rates remarkably below the critical field usually defined as $\alpha = \eta$ that can contribute significantly to discharge inception threshold and behavior in near- and below-critical electric fields.

REFERENCES

[1] J. Dutton, "A survey of electron swarm data," *Journal of Physical and Chemical Reference Data*, vol. 4, no. 3, pp. 577–856, 1975. [Online]. Available: http://dx.doi.org/10.1063/1.555525

[2] Y. Tanaka, "Prediction of dielectric properties of N_2/O_2 mixtures in the temperature range of 3003500k," *Journal of Physics D: Applied Physics*, vol. 37, no. 6, p. 851, 2004. [Online]. Available: http://stacks.iop.org/0022-3727/37/i=6/a=008

[3] M. Seeger, G. Naidis, A. Steffens, H. Nordborg, and M. Claessens, "Investigation of the dielectric recovery in synthetic air in a high voltage circuit breaker," *Journal of Physics D: Applied Physics*, vol. 38, no. 11, p. 1795, 2005. [Online]. Available: http://stacks.iop.org/0022-3727/38/i=11/a=020

[4] M. Capitelli, C. M. Ferreira, B. F. Gordiets, and A. I. Osipov, *Plasma Kinetics in Atmospheric Gases*. Springer-Verlag Berlin Heidelberg, 2000. [Online]. Available: http://dx.doi.org/10.1007/978-3-662-04158-1

[5] S. Pancheshnyi, "Effective ionization rate in nitrogenoxygen mixtures," *Journal of Physics D: Applied Physics*, vol. 46, no. 15, p. 155201, 2013. [Online]. Available: http://stacks.iop.org/0022-3727/46/i=15/a=155201

[6] H. F. A. Verhaart and P. C. T. van der Laan, "The influence of water vapor on avalanches in air," *Journal of Applied Physics*, vol. 55, no. 9, pp. 3286–3292, 1984. [Online]. Available: http://dx.doi.org/10.1063/1.333364

[7] G. Hagelaar and L. Pitchford, "Solving the Boltzmann equation to obtain electron transport coefficients and rate coefficients for fluid models," *Plasma Sources Science and Technology*, vol. 14, no. 4, pp. 722–733, NOV 2005. [Online]. Available: http://dx.doi.org/10.1088/0963-0252/14/4/011

[8] L. C. Pitchford, J. P. Boeuf, and W. L. Morgan, "User-friendly boltzmann code for electrons in weakly ionized gases," in *IEEE Conference Record - Abstracts. 1996 IEEE International Conference on Plasma Science*, June 1996, pp. 154–.

[9] BOLSIG+ Electron Boltzmann Solver. [Online]. Available: www.bolsig.laplace.univ-tlse.fr

[10] LXCAT Plasma Data Exchange Project. [Online]. Available: www.lxcat.net

[11] S. Pancheshnyi, B. Eismann, G. Hagelaar, and L. Pitchford. Computer code ZDPlasKin (University of Toulouse, LAPLACE, CNRS-UPS-INP, Toulouse, France, 2008). [Online]. Available: www.zdplaskin.laplace. univ-tlse.fr

[12] L. C. Pitchford, L. L. Alves, K. Bartschat, S. F. Biagi, M. C. Bordage, A. V. Phelps, C. M. Ferreira, G. J. M. Hagelaar, W. L. Morgan, S. Pancheshnyi, V. Puech, A. Stauffer, and O. Zatsarinny, "Comparisons of sets of electronneutral scattering cross sections and swarm parameters in noble gases: I. argon," *Journal of Physics D: Applied Physics*, vol. 46, no. 33, p. 334001, 2013. [Online]. Available: http://stacks.iop.org/0022-3727/46/i=33/a=334001

[13] L. L. Alves, K. Bartschat, S. F. Biagi, M. C. Bordage, L. C. Pitchford, C. M. Ferreira, G. J. M. Hagelaar, W. L. Morgan, S. Pancheshnyi, A. V. Phelps, V. Puech, and O. Zatsarinny, "Comparisons of sets of electronneutral scattering cross sections and swarm parameters in noble gases: Ii. helium and neon," *Journal of Physics D: Applied Physics*, vol. 46, no. 33, p. 334002, 2013. [Online]. Available: http://stacks.iop.org/0022-3727/46/i=33/a=334002

[14] M. C. Bordage, S. F. Biagi, L. L. Alves, K. Bartschat, S. Chowdhury, L. C. Pitchford, G. J. M. Hagelaar, W. L. Morgan, V. Puech, and O. Zatsarinny, "Comparisons of sets of electronneutral scattering cross sections and swarm parameters in noble gases: Iii. krypton and xenon," *Journal of Physics D: Applied Physics*, vol. 46, no. 33, p. 334003, 2013. [Online]. Available: http://stacks.iop.org/0022-3727/46/i=33/a=334003

[15] S. Pancheshnyi, S. Biagi, M. C. Bordage, G. Hagelaar, W. L. Morgan, A. V. Phelps, and L. C. Pitchford, "The lxcat project: Electron scattering cross sections and swarm parameters for low temperature plasma modeling," *Chemical Physics*, vol. 398, pp. 148 – 153, 2012-04 2012. [Online]. Available: http://dx.doi.org/10.1016/j.chemphys.2011.04.020

[16] (May 2014) Phelps database. [Online]. Available: www.lxcat.net/Phelps

[17] (May 2014) SIGLO database. [Online]. Available: www.lxcat.net/Siglo

[18] S. M. Starikovskaia, N. B. Anikin, S. V. Pancheshnyi, D. V. Zatsepin, and A. Y. Starikovskii, "Pulsed breakdown at high overvoltage: development, propagation and energy branching," *Plasma Sources Science and Technology*, vol. 10, no. 2, p. 344, 2001. [Online]. Available: http://stacks.iop.org/0963-0252/10/i=2/a=324

[19] A. V. Phelps and L. C. Pitchford, "Anisotropic scattering of electrons by n_2 and its effect on electron transport," *Phys. Rev. A*, vol. 31, pp. 2932–2949, May 1985. [Online]. Available: http://dx.doi.org/10.1103/PhysRevA.31.2932

[20] L. Pitchford et al., "Comparisons of sets of electronneutral scattering cross sections and calculated swarm parameters in O_2 and N_2," in *Proc. APS Meeting Abstracts*, October 2012. [Online]. Available: http://meetings.aps.org/link/BAPS.2012.GEC.PR1.88

[21] D. Goodwin, "An Open-Source, Extensible Software Suite for CVD Process Simulation," in *Proc. Chemical vapor deposition XVI and EUROCVD 14*. Pennington, NJ: Electrochemical Society, 2003, pp. 155–162.

[22] (May 2014) Viehland database. [Online]. Available: www.lxcat.net/Viehland

Alise Chachereau followed preparatory classes to the French Grandes Ecoles at Lycée Descartes in Tours, France. She received the master's degree from the Ecole Centrale de Lyon in 2013, after doing her final internship at ABB Corporate Research Center in Baden-Dätwill, Switzerland. She is currently pursuing the Ph.D. degree at the High Voltage Laboratory of ETH Zurich, Switzerland.

Sergey Pancheshnyi received the master's degree from the Moscow Institute of Physics and Technology (MIPT), Russia, in 1998, where he also obtained the Ph.D. degree in plasma physics and chemistry in 2001. He obtained the Habilitation thesis at the University of Toulouse, France, in 2007. He began working in scientific research in 1995 at MIPT and continued at CNRS, France in 2004. In 2010–2011 he was running a high-tech startup company in the Netherlands, then joined the Swiss Corporate Research Center of ABB as Principal Scientist. At ABB his work focuses on non-thermal plasmas and insulation systems.